

Magnet Design Report

Corrector magnet C8

| Author | Checked by – date | Approved by – date |
|-------------------|-------------------|--------------------|
| Davide Castronovo | | |
| | | |
| | | |

Table of Contents

| | | |
|-----|----------------------------------------------|----|
| 1 | INTRODUCTION..... | 3 |
| 1.1 | ACRONYMS AND ABBREVIATIONS..... | 3 |
| 2 | REQUIREMENTS AND CONSTRAINTS | 3 |
| 3 | MAGNETS DESIGN..... | 4 |
| 3.1 | MAGNET PARAMETERS..... | 4 |
| 3.2 | MAGNET YOKE LAYOUT | 5 |
| 3.3 | COIL DESIGN..... | 5 |
| 4 | MAGNETIC FIELD CALCULATIONS..... | 6 |
| 4.1 | 3D SIMULATIONS..... | 6 |
| 4.2 | HARMONIC ANALYSIS..... | 6 |
| 4.3 | FRAME GEOMETRY OPTIMIZATION | 7 |
| 4.4 | TWO-PLANE CORRECTOR | 7 |
| 5 | C8 SUMMARY | 9 |
| 5.1 | CONCEPTUAL 3D MODEL..... | 9 |
| 5.2 | C8 MAGNETIC PERFORMANCES | 10 |
| 6 | ANNEX..... | 10 |
| 6.1 | MATERIAL USED FOR MAGNETIC SIMULATIONS | 10 |
| 6.2 | CORRECTOR MODEL..... | 10 |

1 INTRODUCTION

The last part of the Accelerator-to-Target (A2T) section of the ESS accelerator contains four high-strength combined horizontal and vertical plane corrector magnets for beam trajectory steering. These correctors are normal-conducting and operate in DC mode.

This document describes the conceptual design of these corrector magnets, which are referred to as type C8.

1.1 ACRONYMS AND ABBREVIATIONS

| Acronym | Explanation |
|---------|--------------------------|
| DC | Direct Current |
| PC | Power Converter |
| GFR | Good Field Region |
| FFT | Fast Fourier Transform |
| GUI | Graphical User Interface |
| CAD | Computer Aided Design |
| ABS | Absolute Value |
| Pw | Power |

2 REQUIREMENTS AND CONSTRAINTS

The ESS corrector C8 has the overall dimensions mainly driven by the Linac layout. In particular, the overall length must be lower than 350 mm.

The full aperture of this corrector is equal to those of the quadrupole Q8, which is at least 126 mm.

Even if the correctors will be window frame magnets, the required field quality $\Delta|Bydz(x)|/|Bydz(0)|$ has to be better than 4 %.

To minimize as much as possible the eddy current in the iron to allow possible feedback operations, the yokes will be made of laminated steel sheets with a thickness of 1 mm.

A further constraint, coming from the operation mode of the power converter, is the maximum current value which is fixed at maximum 16 A.

The solid copper wire must have a cross-section of 10 mm² in order to maintain the maximum current density smaller than 1.6 A/mm².

Table 1 lists the requirements for C8 corrector.

Table 1: C8 DOORS requirements

| Requirements for magnet type C8 | | | | |
|----------------------------------------|-----------------------------------------------------|--------|--------------|-------------|
| ID | Parameter | | value | unit |
| 4603 | Full aperture | \geq | 126 | mm |
| 4602 | Overall length | \leq | 350 | mm |
| 4619 | Nominal magnetic field integral | $=$ | 100 | Gm |
| 4620 | Operating range | $=$ | ± 100 | Gm |
| 4621 | Maximum magnetic field integral | \geq | 110 | Gm |
| 4624 | Good field region radius | \geq | 42 | mm |
| 4622 | Integrated field quality $\text{abs}(\Delta B/B_0)$ | $<$ | 4 | % |

3 MAGNETS DESIGN

3.1 MAGNET PARAMETERS

The proposed design of C8 is combined horizontal and vertical corrector window frame. The electromagnetic simulations and optimizations used the software packages VF Opera 3D (Tosca) and Matlab. Table 2 lists the magnets parameters and performances.

Table 2: Magnets parameters and performances calculated by VF Opera 3D.

| Parameters | Value | unit |
|--------------------------------------------|--------------|-------------|
| Full aperture | 130 | mm |
| Yoke overall width and height | 270 | mm |
| Good field region radius r_0 | 42 | mm |
| Yoke length | 300 | mm |
| Coils overall length | 346 | mm |
| Magnetic length L_{eff} at nominal I_c | 465 | mm |
| Maximum integrated gradient | 139.5 | Gm |
| Integrated field quality $(\Delta B/B_0)$ | < 4 | % |
| Harmonic contents at r_0 | < 4 | % |
| Inductance | 68 | mH |

3.2 MAGNET YOKE LAYOUT

The magnetic circuit consists of four identical quadrants that are precisely bolted together by means of dowel pins.

In order to allow a possible feed-back mode of operation, the yoke quadrants are made of laminated steel sheets of 1 mm thickness that are glued together. The material curve $B(H)$ used for the magnetic field calculations is the VF Opera “tenten” (see Table 8). A packing factor of 97% (low margin respect the typically value of 98%) has been assumed for the calculations.

Table 3 lists all yoke parameters. Note that the yoke weight was calculated by the typically value of the packing factor, which is 0.98.

Table 3: Yoke parameters

| Parameters | | unit |
|---------------------------------------------------|------------------|------|
| Type | Laminated | mm |
| Material | Low carbon steel | mm |
| Packing factor | ≥ 97 | mm |
| Yoke width / height | 270 | mm |
| Yoke length | 300 | mm |
| Yoke mass (calculated by $0.98 \cdot \rho_{Fe}$) | 56 | kg |

3.3 COIL DESIGN

The coils are made of rectangular pre-insulated solid copper wire with a cross section of 3.15×3.55 mm and a conducting area of 10.63 mm^2 . The coils shall be vacuum-impregnated using radiation-resistant thermosetting epoxy resin and the final insulation has to withstand a test voltage of 5 kV.

The coil parameter calculations assumed a resistivity of $1.72 \times 10^{-8} \Omega\text{m}$ at 20°C . The relatively low current density allows coil cooling by natural air-convection. However each coil will be equipped with thermal switched for protection against accidental overheating.

Table 4 lists all coils parameters and an overview of all relevant power converter parameters.

Table 4: Coil parameters

| Parameters | | unit |
|----------------------------------------|-------------|-------------------|
| Type | Racetrack | |
| Cooling | Air-cooled | |
| Number of turns for one coil | 210 | # |
| Number of turns on width | 6 | # |
| Number of turns on height for one coil | 35 | # |
| Conductor cross section | 3.15 x 3.55 | mm |
| Space between coils and yoke | 3 | mm |
| Maximum current density j | 1.47 | A/mm ² |
| Conductor length for one coil | 161.2 | m |
| Resistance for one coil | 253.5 | mΩ |
| Coil overall length | 346 | mm |
| Coil mass | 15.6 | kg |
| PC Maximum current I_{MAX} | 16 | A |
| Maximum voltage | 8.1 | V |
| Maximum power dissipation | 130 | W |

4 MAGNETIC FIELD CALCULATIONS

4.1 3D SIMULATIONS

Since the correctors have a large aperture gap, more than half of the yoke length, 2D simulations and pre-design calculations cannot give reliable results. Therefore all the magnetic field calculations have been done using VF Opera 3D

For calculating each one-plane corrector, the Opera 3D models use the transversal symmetries on the plane ZX and on the plane YZ, plus the longitudinal symmetry on the plane XY. In this way the simulated model is one-eighth (1/8th) of the whole magnet.

For calculating both the correctors (two-plane corrector), the Opera 3D models use only the longitudinal symmetry on the plane XY. In this way the simulated model is one-half of the whole combined magnets.

4.2 HARMONIC ANALYSIS

As done for the quadrupoles, the harmonic content of the magnetic flux density is evaluated calculating the FFT components of the integrals of the field around a cylinder defined by the GFR radius.

4.3 FRAME GEOMETRY OPTIMIZATION

Since for the corrector the required field quality $\Delta|B_{yz}(x)|/|B_{yz}(0)|$ has to be better than 4 %, a normal window frame geometry is not sufficient. In order to obtain the required field homogeneity, the magnet has a frame shape with trapezoidal poles. The frame geometry and dimensions have been optimized by 3D simulations at the maximum current.

Figure 1 shows the adopted Opera 3D models while Table 5 lists the harmonic components in both cases (without and with “poles”).

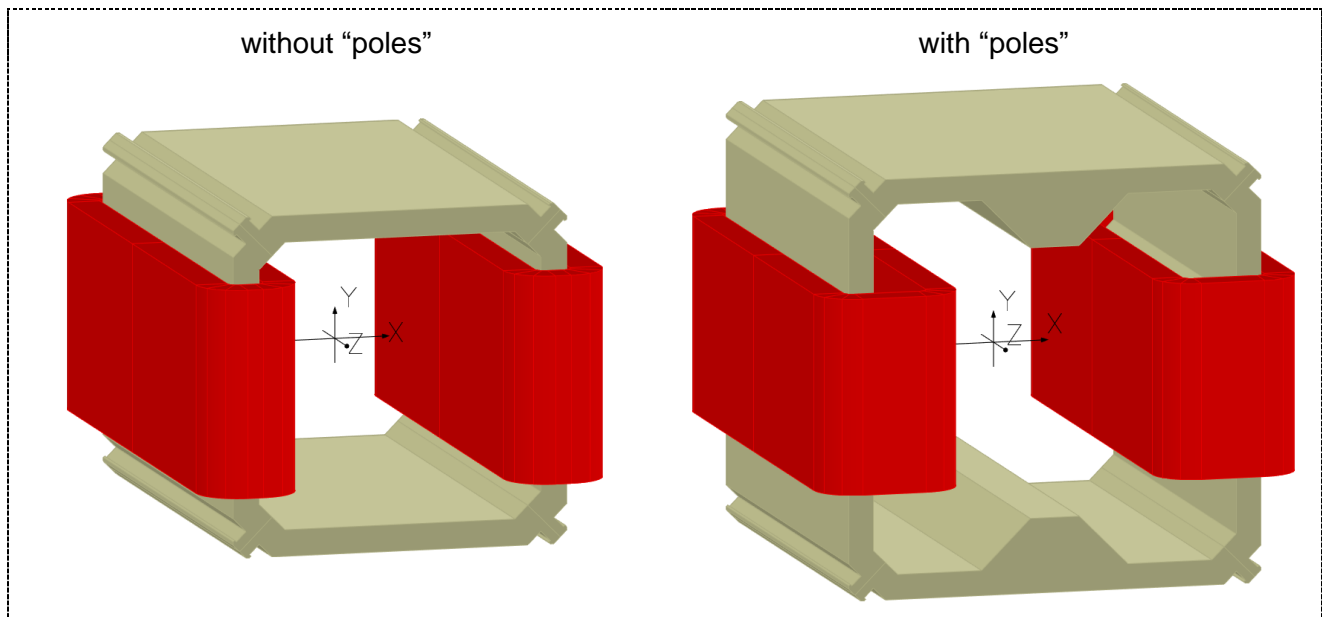


Figure 1: C8 Opera 3D models with and without the “poles” geometries

Table 5: C8 performances and harmonic components with and without “poles” geometries at 16 A

| Corrector | $\int B_0$ [Gm] | L_{eff} [mm] | $\Delta B /\int B_0$ [%] | $\int B_3/\int B_1$ [%] | $\int B_5/\int B_1$ [%] |
|------------------|-----------------|----------------|--------------------------|-------------------------|-------------------------|
| without | 112.5 | 439.3 | 5.41 | 5.54 | 0.63 |
| with | 111.3 | 464.7 | 4.03 | 3.32 | 1.25 |

4.4 TWO-PLANE CORRECTOR

If the coils of both planes are energized the field distribution inside the yoke is asymmetrical and has a higher maximum value compared to the case of a single plane excitation.

In order to improve the comparison between the two cases (one corrector and both correctors energized), the Opera 3D models are the same with and without the excitation of the other pair of coils. This behavior has been studied for a current of 16 A. Table 6 lists the magnetic performances in both cases. To note that the values can be a little bit

different, if compared with that of Table 6, due to the model without the transversal boundary conditions.

Table 6: C8 magnetic performances at 16 A; only CH and combined CH and CV excitations

| Corrector | $\int B_0$ [Gm] | L_{eff} [mm] | $\Delta B / \int B_0$ [%] | $\int B_3 / \int B_1$ [%] | $\int B_5 / \int B_1$ [%] |
|------------------|-----------------|----------------|---------------------------|---------------------------|---------------------------|
| only CH | 111.3 | 464.9 | 3.980 | 2.99 | 1.12 |
| CH & CV | 111.2 | 464.4 | 3.987 | 4.23 | 1.59 |

It is possible to observe that the excitation of both planes increases the harmonic components B3 and B5. Otherwise, the magnetic length L_{eff} , the integrated field and the field homogeneity are not affected.

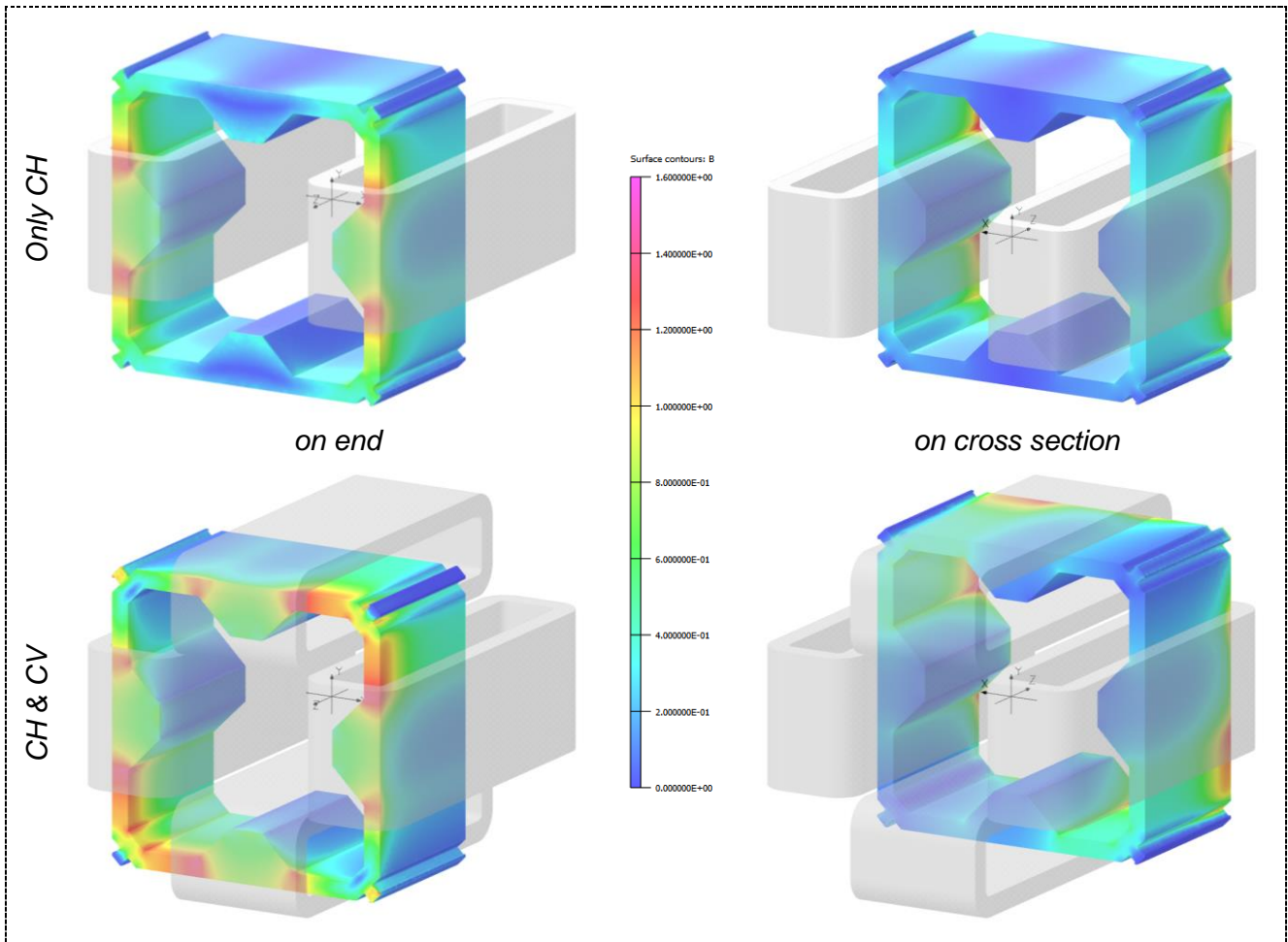


Figure 5: B field distributions at 16 A; colored bar from 0 to 1.6 T

In both the cases the maximum field in the middle cross section is lower than 0.6 T, which is quite distant from the iron saturation value (1.6 T). On the other hands, the field on the transversal end surfaces of the iron is higher due to the coils proximity.

5 C8 SUMMARY

5.1 CONCEPTUAL 3D MODEL

The C8 conceptual model include the yoke quadrants and the coils overall shape.

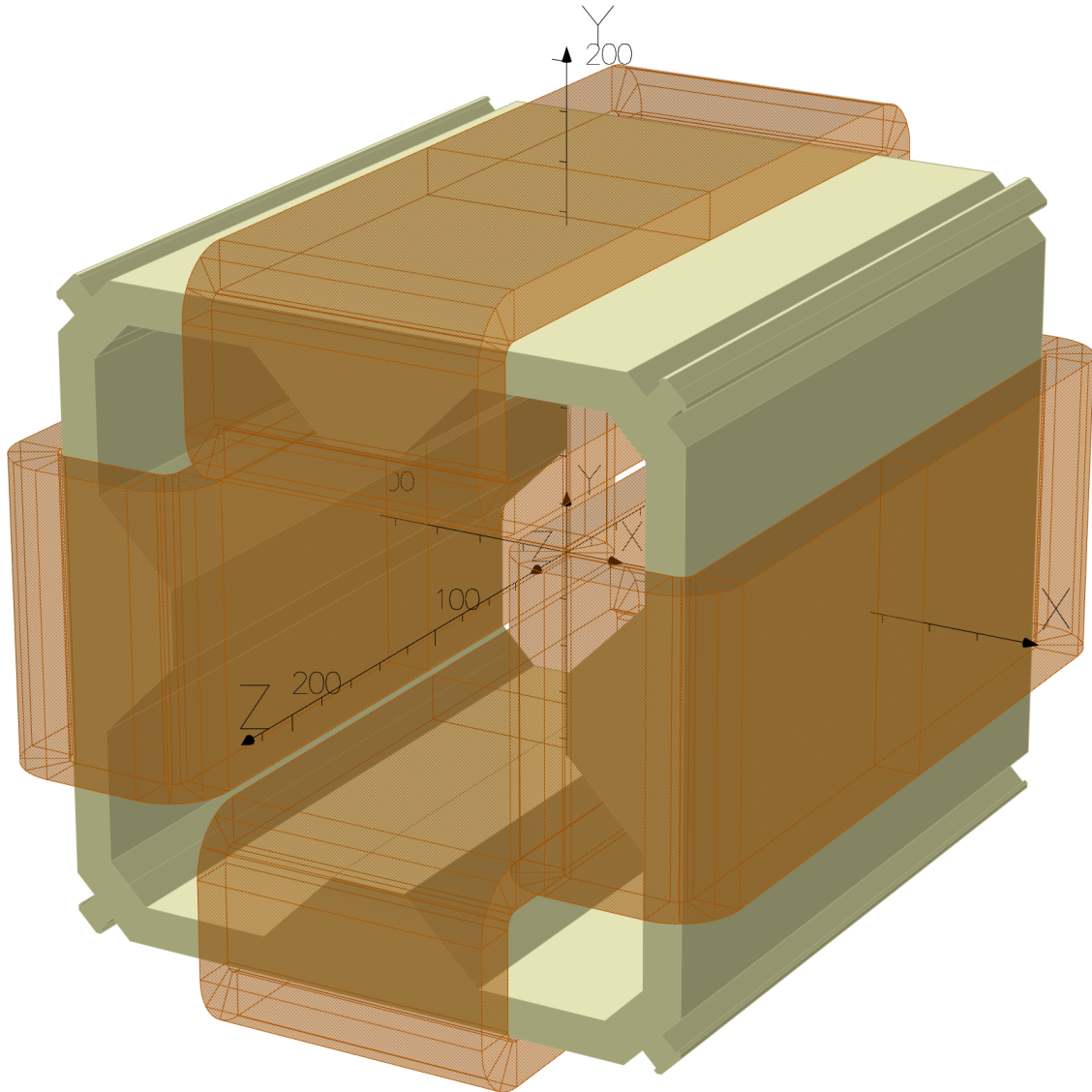


Figure 6: C8 conceptual model

The yoke frame could be modified in order to increase the possible supporting surface and defined the closing system.

5.2 C8 MAGNETIC PERFORMANCES

In order to obtain consistent results, the C8 magnetic performances are calculated by Opera 3D for several excitation current values on the same 3D model and with the same post processing actions. Table 7 lists the C8 magnetic performances.

Table 7: C8 magnetic performances

| | Curr [A] | $\int B$ [Gm] | L_{eff} [mm] | sat [%] | $\Delta \int B / \int B0$ [%] | $\int B_3 / \int B_1$ [%] | $\int B_5 / \int B_1$ [%] |
|---------------|-----------------|---------------------------------|----------------------------------|----------------|-------------------------------------------------|---------------------------------------------|---------------------------------------------|
| | 16 | 111.35 | 464.9 | -0.08 | 4.03 | 2.98 | 1.14 |
| | 15.8 | 109.96 | 464.9 | -0.07 | 4.03 | 2.98 | 1.14 |
| | 14.4 | 100.24 | 464.6 | -0.06 | 4.03 | 2.98 | 1.14 |
| nominal range | 12 | 83.55 | 465.1 | -0.03 | 4.03 | 2.98 | 1.14 |
| | 8 | 55.71 | 465.2 | -0.02 | 4.03 | 2.98 | 1.14 |
| | 4 | 27.86 | 465.2 | 0 | 4.03 | 2.98 | 1.14 |
| | 0 | nan | nan | nan | nan | nan | nan |

6 ANNEX

6.1 MATERIAL USED FOR MAGNETIC SIMULATIONS

The material used for the magnetic simulation is based on the Opera “tenten” data. Table 8 lists the relative $B(H)$ data.

Table 8: $B(H)$ data of the steel type used for magnetic field simulation

| B [Gauss] | H [Oersted] |
|------------------|--------------------|
| 0 | 0 |
| 5757 | 2.09 |
| 6800 | 2.5 |
| 7918 | 3.02 |
| 8949 | 3.63 |
| 9921 | 4.365 |
| 10821 | 5.248 |
| 11640 | 6.31 |
| 12373 | 7.586 |
| 13021 | 9.12 |
| 13586 | 10.96 |
| 14074 | 13.18 |
| 14494 | 15.85 |
| 15171 | 22.91 |
| 15451 | 27.54 |
| 15955 | 39.8 |
| 16455 | 57.54 |
| 17019 | 83.18 |
| 17679 | 120.23 |
| 18045 | 144.5 |
| 18432 | 173.8 |
| 18831 | 208.9 |
| 19236 | 251.2 |
| 19636 | 301.99 |
| 20022 | 363.08 |
| 20384 | 436.5 |
| 20713 | 524.8 |
| 21003 | 630.95 |
| 21251 | 758.7 |
| 21461 | 912 |
| 21646 | 1096.5 |
| 21869 | 1318.3 |
| 22137 | 1584.9 |
| 22458 | 1905 |

6.2 CORRECTOR MODEL

The quadrupole 3D model could be exported in the step file format. The following page reports the base drawing of the model.

